LIQUID–LIQUID PHASE SEPARATION IN MULTICOMPONENT POLYMER SYSTEMS. XXVI. BLENDS OF TWO POLYDISPERSE POLYMERS

Karel SOLC[a],* and Ronald KONINGSVELD[b]

[a] *Michigan Molecular Institute, Midland, MI 48640, U.S.A.*
[b] *Max-Planck Institute for Polymer Research, P.O. Box 3148, D-55021, Mainz, Germany*

Dedicated to Dr Blahoslav Sedlacek on the occasion of his 70th birthday.

A method for computing phase diagrams of polydisperse A/B polymer blends is proposed, based on Flory–Huggins–Staverman thermodynamics, and employed to obtain cloud-point curves (CPCs), shadow curves, spinodals and coexistence curves for a series of systems. Often bimodal CPCs and shadow curves result, even for systems with a concentration-independent interaction parameter g. The importance of coexistence curves, as opposed to CPCs, for judging the A/B miscibility, recently observed in polydisperse blends, is confirmed in this study. Particular attention is here paid to the critical state. Analytical relations are derived for the critical point (CP) and the critical slopes of the CPC and shadow curve, as well as for the criterion of CP stability, all in terms of various molar-mass averages of A and B. The latter criterion then yields conditions for the existence of heterogeneous double CPs and triple CPs, important as markers announcing the proximity of a three-phase region. Interestingly, the sign of the critical CPC slope depends solely on the relative magnitude of the r_z/r_w ratios for the two polymers A and B. Hence, a CP located at the CPC's top should not be interpreted as a proof of both polymers' monodispersity. The validity of derived analytical relations is confirmed by numerically computed phase diagrams.

Polymers usually possess a rather broad distribution of molar mass unless special methods are used and great care is taken during their preparation. Yet, the effect of polymer polydispersity on the phase behavior of polymeric systems has been thoroughly examined only for the simplest case, i.e., for solutions of polydisperse homopolymers. Years ago, a numerical computation of phase equilibria in bulk polydisperse polymer mixtures has been reported briefly[1], however, the cloud-point curves (CPCs) had to be obtained by extrapolation of results from several computer runs with various

---

* The author to whom correspondence should be addressed.

non-zero phase-volume ratios. Such a procedure is lengthy, inherently inaccurate, and may obscure some important details of phase diagrams.

A fast direct method for CPC computation in solutions of polydisperse polymers was developed in early seventies[2]. Its adaptation for polydisperse polymer blends, complemented by a series of formulas for the critical state, is presented here; it also provided the basis for a program in the Phase Diagram module, part of the Polymer Software marketed by BIOSYM Technologies, Inc.[3]. Other direct methods for blends were reported recently[4].

In one respect this case is still simple: the system contains only two constituents whose interaction can be described by a single interaction parameter g. However, both of these constituents are now polydisperse, and it is not immediately obvious how to handle the situation which, e.g., gave rise to confusion on some very fundamental questions, such as, whether the critical points here can be stable at all.

In our past work on systems solvent–polydisperse polymer, the most effective approach was to base the analysis on the separation factor σ introduced for polymer solutions by Flory[5]. An analogous method turns out to be beneficial for bulk quasibinary systems as well, although two σ parameters are here required to describe the behavior[1]. The results should allow for a more realistic modeling as well as interpretation of experimental data on polymer–polymer compatibility, typically obtained with polydisperse polymer samples. In addition, this exercise provides the background for analysis of more complex cases such as quasiternary solutions[6] and statistical-copolymer systems[7].

In the next two sections equations for the cloud-point and coexistence curves are derived from the general condition for phase equilibrium in systems obeying the Flory–Huggins–Staverman (FHS) thermodynamics[1,5]. In Section 3 various relations for the critical state are obtained, that are then applied to multiple critical point analysis in Section 4. Finally, Section 5 contains numerically computed phase diagrams for some polydisperse blends, partly confirming the derived relations, partly illustrating some phenomena of general interest.

1. THERMODYNAMIC BACKGROUND

A general expression for ΔG^m, the Gibbs energy of mixing Σn_{Ai} and Σn_{Bj} moles of polymers A and B, respectively, in bulk may be written as[1,5]

$$\Delta G^m / R_g T = \sum_i n_{Ai} \ln \varphi_{Ai} + \sum_j n_{Bj} \ln \varphi_{Bj} + \Gamma \ , \qquad (1a)$$

where $R_g T$ has its usual meaning, n denotes the amount (in mol) and φ the volume fraction, with the letter subscripts A, B referring to the two polymeric constituents, and the running subscripts i, j, if present, specifying each constituent's fractions (i.e., their

components). For instance, φ_{Ai} is the volume fraction of the i-th component of polymer A, and the total volume fraction of A is $\varphi_A = \Sigma\varphi_{Ai}$. The normalized molar mass distribution (MMD) of A is then defined by $w_{Ai} \equiv \varphi_{Ai}/\varphi_A$, the mass fraction of component i in pure constituent A. The system is thought to be built up of N basic volume units (BVU) where $N = \Sigma\, n_{Ai}r_{Ai} + \Sigma n_{Bj}r_{Bj}$; here the relative chain length r_{Kl} is defined as the number of BVU's occupied by a chain l of polymer K, and the volume fraction of such chains in the blend is $\varphi_{Kl} = n_{Kl}r_{Kl}/N$.

Molecular models have been developed that differ by the specific form of the interaction function Γ in Eq. (*1a*). For instance, in the original FHS treatment Γ was assumed to be given by the Van Laar expression

$$\Gamma_{FHS} = g\varphi_B \sum_i n_{Ai}\, r_{Ai} \ , \tag{1b}$$

where the interaction parameter, g, depends solely on temperature, T. Other models make g concentration dependent, and are subject of current research.

The equilibrium condition of equal chemical potentials $\underline{\Delta}\, \mu_{Kl}$ in the two phases (′) and (″) for the l-th component of polymer K leads to the relation

$$\Delta(\underline{\Delta}\mu_{Kl})/(r_{Kl}\, R_g T) = r_{Kl}^{-1}\Delta(\ln \varphi_{Kl}) - \Delta U + \Delta[(g + \varphi_K g_K)\varphi_L^2] = 0 \ , \tag{2}$$

where K, L = A, B, K ≠ L; $g_K \equiv (\partial g/\partial \varphi_K)_{T,\varphi_L}$, Δ stands for the difference between the two phases (e.g., $\Delta\varphi_K = \varphi_K'' - \varphi_K'$), and U is the overall reciprocal number-average chain length,

$$U \equiv \sum_i (\varphi_{Ai}/r_{Ai}) + \sum_j (\varphi_{Bj}/r_{Bj}) = (\varphi_A/r_{A,n}) + (\varphi_B/r_{B,n}) \ , \tag{3}$$

with $r_{K,n}$ being the number-average chain length of the constituent K. From Eq. (*2*) it is obvious that the concept of Flory's separation factor, σ, originally introduced for solutions of polydisperse polymers[5], can be utilized for polymer blends as well if a separate σ is defined for each polymeric constituent[1,6–8],

$$\sigma_K \equiv r_{Kl}^{-1} \Delta (ln \ \varphi_{Kl}) = \Delta U - \Delta[(g + \varphi_K g_K)\varphi_L^2] \ . \tag{4a}$$

Further discussion will be limited to the simplest case where g of Eq. (*1b*) is independent of concentration, i.e., $g_K = 0$.

Following the method well proven for ternary systems[8], we define (i) a symmetrical cloud-point function F independent of g, i.e., independent of temperature, and (ii) a difference function G compactly expressing the effect of interactions g between the two polymers.

The function F is obtained by multiplying the simplified version of Eq. (*4a*) for each constitutent by its ($\varphi_K' + \varphi_K''$), and summing over K,

$$F \equiv \sigma_A(\varphi_A' + \varphi_A'') + \sigma_B(\varphi_B' + \varphi_B'') - 2\Delta U = 0 \ , \tag{5}$$

while G is formed by subtracting the zeroed Eqs (*4a*) written for A and B,

$$G \equiv \sigma_B - \sigma_A + g(\Delta\varphi_A - \Delta\varphi_B) = 0 \ . \tag{6a}$$

The latter relation can be further rearranged: since there is no solvent present in the polymer blend, we have by definition

$$\varphi_A + \varphi_B = \varphi_A' + \varphi_B' = \varphi_A'' + \varphi_B'' = 1 \ , \qquad \text{i.e.,} \qquad \Delta\varphi_A + \Delta\varphi_B = 0 \ , \tag{7a, 7b}$$

and Eq. (*6a*) can be recast as

$$\sigma_B - \sigma_A = 2g \, \Delta\varphi_B \ . \tag{6b}$$

The parameter g is thus proportional to the difference between the two separation factors and inversely proportional to the concentration difference $\Delta\varphi_B$ between the two phases. It may be noted that the functions F and G of Eqs (*5*) and (*6a*) are the bulk polydisperse equivalents of the functions F and G introduced earlier for ternary solutions (cf. Eqs (*4*) and (*5*) of ref.[8]). There is no equivalent to the ternary function H since the solvent is absent from our system.

It is apparent that the two factors σ_A and σ_B are not independent; they have to be compatible with relations (*7*). On a qualitative level, they have to be of opposite signs, $\sigma_A\sigma_B \leq 0$, since enrichment of a phase by one polymer inevitably means impoverishment in terms of the other. The detailed form of this condition will be discussed later.

2. CLOUD-POINT AND COEXISTENCE CURVES

In thermodynamics of quasibinary polymer solutions the most common type of phase diagram contains the *cloud-point curve* (sometimes with its conjugate counterpart *shadow curve*) specifying the dependence of the cloud point temperature on polymer concentration. It can be obtained relatively easily, both experimentally and theoretically, and it is convenient for characterization of the dissolved polymer sample. Only rarely would one also see plotted so-called *coexistence curves*, tracing for one solution of a particular composition the changes in concentrations of coexisting phases with changing temperature[9–11]. On the other hand, for bulk polymer blends the interest may well be shifted towards the latter curves since, from the point of view of blend performance, one often desires to know the phase behavior of a particular polymer mixture over a range of temperatures that could affect its ultimate properties[4]. In the following paragraphs, both subjects are briefly recalled.

The computation of the CPC is fairly simple: Since the amount of the separated incipient phase here approaches zero, the composition of the unindexed principal phase is known, being identical to that of the original mixture before phase demixing. With changed notation [$('') \rightarrow (^*)$ for the incipient phase, and $(') \rightarrow (\ )$ for the principal phase], Eq. (*4a*) yields[2,8]

$$\varphi^*_{Ki} = \varphi_K\, w_{Ki}\, \exp\,(\sigma_K r_{Ki}) \tag{4b}$$

and the remaining needed function B^* can be defined from Eqs (*7*) as

$$B^* \equiv \varphi^*_A + \varphi^*_B - 1 = \varphi_A W^*_A(\sigma_A) + \varphi_B W^*_B(\sigma_B) - 1 = 0 \ , \tag{8a}$$

where, for the known MMD's of A and B, the quantity $W^*_K(\sigma_K) \equiv \Sigma w_{Ki} \exp\,(\sigma_K r_{Ki})$ is a function of only σ_K.

Since the CPC in T vs φ_B coordinates has one degree of freedom, one can select the value for one of the relevant variables (T, φ_B, σ_A, σ_B) as the CPC's parameter. A good option seems to be one of the separation factors, say σ_B, whose value is a measure of the distance of the cloud point from the critical point (CP); note that at the CP, $\sigma_A = \sigma_B = 0$. The computation can be accomplished in a single iteration cycle: e.g., for a $\sigma_B > 0$, a negative trial value of the other factor, σ_A, is chosen, φ_B is computed from Eq. (*8a*) as

$$\varphi_B = [1 - W^*_A(\sigma_A)]/[W^*_B(\sigma_B) - W^*_A(\sigma_A)] \tag{9}$$

and with the incipient-phase concentrations φ_{Ki}^* expressed from Eq. (*4b*), the F of Eq. (*5*) is evaluated. The correct value of σ_A, zeroing the function F is found by trial and error. The parameter g (or T) is calculated in the end from Eq. (*6b*). It is apparent that $\sigma_B > 0$ will generate only a part of the CPC; the rest of it requires setting $\sigma_B < 0$. On the whole, the computation of the CPC for a bulk quasibinary polymer mixture is no more difficult than that for a polydisperse homopolymer dissolved in a solvent.

Somewhat more involved is the computation of coexistence curves displaying the fate of a particular mixture of polymers A and B, as it is taken by varying its temperature through the cloud point and deeper into the two-phase region. Then of course neither one of the two coexisting-phase compositions is known; they are, however, related by the volume-conservation Eq. (*10*). The additional parameter varying with the extent of penetration into the two-phase region is the phase-volume ratio, $R \equiv V''/V'$, where V' and V'' are the volumes of the respective phases. Assuming volume additivity upon demixing, each component's concentrations have to comply with the relation

$$\varphi_{Ki}' + R\varphi_{Ki}'' = (R + 1)\varphi_{Ki} \qquad (10)$$

that, combined with Eq. (*4a*), permits calculation of each phase's composition in terms of σ_K and R; e.g.,

$$\varphi_K' = \varphi_K(R + 1) \sum \frac{w_{Ki}}{1 + R \exp(\sigma_K r_{Ki})} \ . \qquad (11)$$

A convenient form of the testing function B is then, e.g., the relation (*7a*) written for the phase (′)

$$B' \equiv \varphi_A \sum \frac{w_{Ai}}{1 + R \exp(\sigma_A r_{Ai})} + \varphi_B \sum \frac{w_{Bj}}{1 + R \exp(\sigma_B r_{Bj})} - \frac{1}{1 + R} = 0 \ . \qquad (8b)$$

The computation procedure now differs from that used for CPCs. Since the desired result is the coexistence curve for a blend of a particular composition, φ_A and φ_B of Eq. (*8b*) have to be kept constant, and the selected value of another parameter will determine the position of the computed point on the coexistence curve. Unlike in the CPC calculation, in this case there seems to be no way of avoiding double iteration. For instance, one may select a value for R, and search by trial and error for values of σ_A and σ_B that would satisfy B' of Eq. (*8b*) and F of Eq. (*5*). As before, the parameter g is determined last from Eq. (*6b*) after the iteration of σ_A and σ_B has been completed. A similar scheme was used for an α/β statistical copolymer system characterized by a two-dimensional distribution of chain length and composition[7].

The cloud point can also be obtained as a special point of the coexistence curve[1]. Our version of B, B' of Eq. (*8b*), premultiplied by R, is suitable only for mimicking the limit for $R \to \infty$ that produces the "supercritical" portion of the CPC. It is apparent that for the "subcritical" part requiring the limit for $R \to 0$, the condition (*8b*) becomes trivially satisfied and thus useless. Here an alternative criterion B'' formulated for the phase (''') would be required for computation. While the direct CPC calculation via B^* of Eq. (*8a*) is much simpler and more accurate, the limit approach described here and in ref.[1] offers a good consistency test for the two programs.

For some tasks a preferred alternative to variables σ_K is their transformed version η and ξ, originally introduced for ternary solutions[8],

$$\sigma_A = \pm (\eta^2/\xi^2)^{1/2} \ , \qquad \sigma_B = \mp \ (\eta^2\xi^2)^{1/2} \qquad (12a)$$

or

$$\xi^2 = \sigma_B/\sigma_A \ , \qquad \eta^2 = \sigma_A\sigma_B \ . \qquad (12b)$$

Since for polymer blends σ_A and σ_B have to be of opposite signs, both η^2 and ξ^2 are here negative. Advantages of working with ξ and η are:

a) There is just one variable, η^2, acting as a measure of the distance from the CP, and approaching zero at the CP. Hence, taking the limit of various functions at the CP is simpler.

b) The second variable, ξ^2, on the other hand, typically stays non-zero even at the CP, and changes very little along the CPC (certainly much less than σ_A, σ_B or η^2 do); hence its correct final value from one iteration provides a good starting point of iteration for the neighboring point.

c) ξ^2 characterizes for a given chain length the relative fractionation efficiency for polymer B over that for A, with $|\xi^2| > 1$ indicating a sharper separation for B than for A. Also, its critical value affects the critical binodal direction in the multidimensional composition space (see below).

3. CRITICAL STATE

Since F converges to zero as η^3, we work with its reduced form* $\overline{F} \equiv 6F/\eta^3$. Its expansion into an η power series, reported for strictly ternary systems as Eq. (*16*) of

---

* In the past definitions of the modified function $\overline{F}$ for ternary systems[8,12], the solute concentration φ in

ref.[12], turns out to be equally applicable for polydisperse blends if the second negative solvent-related term is omitted and the moments are properly redefined. The expanded form becomes

$$\bar{F} = 6 \sum_{k=0}^{\infty} \frac{k+1}{(k+3)!} \{ r^{k+2} \xi^{k+3} \} \eta^k \, , \tag{13}$$

where the over-all statistical moments { } are now taken over all components of the two polymeric constituents,

$$\{ r^m \xi^n \} \equiv \varphi_A \xi^{-n} \sum_i w_{Ai} \, r_{Ai}^m + \varphi_B \xi^n \sum_j w_{Bj} \, r_{Bj}^m \, . \tag{13a}$$

Alternatively, the over-all moments { } can be transcribed as averages ⟨ ⟩ over two constituents,

$$\{ r^m \, \xi^n \} \equiv \langle \mu_m \xi^n \rangle = \varphi_A \xi^{-n} \mu_{A,m} + \varphi_B \xi^n \mu_{B,m} \tag{13b}$$

in terms of the regular statistical moments, $\mu_{K,m}$, of each constituent's chain-length distribution, where

$$\mu_{K,m} = \sum_i w_{Ki} \, r_{Ki}^m \, , \quad K = A,B \, . \tag{13c}$$

Consistently with Eq. (20) of ref.[12] for ternary systems, the G function of Eq. (6a) is expanded as

$$\bar{G} \equiv G \xi / \eta = \xi^2 - 1 + \xi g \sum_{m=1}^{\infty} \frac{\eta^{m-1}}{m!} \left[\varphi_A \xi^{-m} \mu_{A,m} - \varphi_B \xi^m \mu_{B,m} \right] \, , \tag{14}$$

whereas the condition (8a) yields

---

the denominator was inadvertently omitted (see the paragraph above Eq. (18a) in ref.[8] and above Eq. 16 in ref.[12]); the correct form should have been $\bar{F} = 6F/(\varphi \eta^3)$. One of us (K.S.) thanks Dr Y.-H. Huang for calling his attention to this error. Fortunately, this oversight has had no effect on subsequent formulas and conclusions since the roots of $\bar{F}$ stay unchanged. In the present paper φ does not appear since it is unity.

$$\mathcal{B} \equiv B^*/\eta = \sum_{m=1}^{\infty} \frac{\eta^{m-1}}{m!} \left[\varphi_A \xi^{-m} \mu_{A,m} + \varphi_B \xi^m \mu_{B,m} \right] . \tag{15}$$

Two critical functions are now obtained as limits for $\eta^2 \to 0$ of the expanded equilibrium functions (13) and (14)

$$F \equiv \lim_{\eta \to 0} \mathcal{F} = \{ r^2 \xi_c^3 \} = \langle r_z r_w \xi_c^3 \rangle = 0 , \tag{16a}$$

$$G \equiv \lim_{\eta \to 0} \mathcal{G} = \xi_c^2 - 1 + g_c (\varphi_{A,c} r_{A,w} - \xi_c^2 \varphi_{B,c} r_{B,w}) = 0 , \tag{16b}$$

where the subscript c denotes the critical values of the variables, and the statistical moments over the chain-length distribution of each constituent have been replaced by more familiar weight- and z-averages, using the identities $\mu_{K,1} \equiv r_{K,w}$ and $\mu_{K,2} \equiv r_{K,w} r_{K,z}$. The third critical relation comes from the condition (15):

$$B \equiv \lim_{\eta \to 0} \mathcal{B} = \langle r_w \xi_c \rangle = 0 . \tag{16c}$$

For ensuing discussion it is convenient to abbreviate the ratios of two consecutive chain-length averages for the same constituent K as a subscripted $\zeta_K \geq 1$. For instance, $\zeta_{A,z+1} \equiv r_{A,z+1}/r_{A,z}$, or, in general,

$$\zeta_{K,t+1} \equiv r_{K,t+1}/r_{K,t} . \tag{17a}$$

Equations (16a) and (16c) can be solved for the critical values of the parameter ξ^2 and the concentration φ_B,

$$\xi_c^2 = -\rho_{A,z}/\rho_{B,z} , \tag{18a}$$

$$\varphi_{B,c} = \rho_{A,q} / (\rho_{A,q} + \rho_{B,q}) , \tag{18b}$$

where the square-root chain-length averages ρ_K are defined as

$$\rho_{K,z} \equiv (r_{K,z})^{1/2} \ , \qquad \rho_{K,q} \equiv r_{K,w}/(r_{K,z})^{1/2} \equiv \rho_{K,z}/\zeta_{K,z} \ . \qquad (18c)$$

Finally, substituted into Eq. (*16b*), these relations yield the critical value of the inter-action parameter as

$$g_c = \frac{(\rho_{A,z} + \rho_{B,z})\,(\rho_{A,q} + \rho_{B,q})}{2r_{A,w}r_{B,w}} \ . \qquad (18d)$$

The relations for $\varphi_{B,c}$ and g_c, Eqs (*18b*) and (*18d*), are equivalent to the results by Koningsveld et al. obtained earlier[1,13] with the aid of the Gibbs method of spinodal and critical determinants. If one of the constituents is a solvent, the relations reduce to the results obtained years ago by Stockmayer[14].

The critical slope of the CPC is obtained from the differential of $\overline{G}$ function (see Appendix 1) as

$$2\left.\frac{\mathrm{d}g}{\mathrm{d}\varphi_B}\right|_c = \left(\rho_{A,q}^{-1} + \rho_{B,q}^{-1}\right)^2\left(\zeta_{A,z}^{-1} - \zeta_{B,z}^{-1}\right) \ . \qquad (18e)$$

Thus, it can be either positive or negative, depending on whether the ratio $r_z/r_w \equiv \zeta_z$ is smaller or greater for the polymer A, relative to that of B. Note that if the ratios r_z/r_w for both A and B are the same, critical slope will be zero, behaving as if the two constituents were monodisperse. Hence, in polymer blends the location of their CP at the maximum (or minimum) of their CPC must not be interpreted as an indication of their monodispersity. Furthermore, if A is indeed monodisperse and B is not, the slope $(\mathrm{d}g/\mathrm{d}\varphi_B)_c$ has to be positive; say, for an UCST system, this condition then places the CP on the right descending branch of the CPC in T vs φ_B coordinates, a pattern well known from the past. For this case the symmetric relation (*18e*) reduces to the result derived earlier (Eq. (*11*) of ref.[2]).

The critical slope of the shadow curve is tied to that of the CPC, Eq. (*18e*), by the trivial relation

$$\left.\frac{\mathrm{d}g}{\mathrm{d}\varphi_B^*}\right|_c = \left.\frac{\mathrm{d}g}{\mathrm{d}\varphi_B}\right|_c \times \left.\frac{\mathrm{d}\varphi_B}{\mathrm{d}\varphi_B^*}\right|_c \ , \qquad (18f)$$

where, from Eq. (*4b*), the latter derivative can be expressed as

$$\left.\frac{\mathrm{d}\varphi_B}{\mathrm{d}\varphi_B^*}\right|_c = \left(1 + \varphi_{B,c}r_{B,w}\left.\frac{\mathrm{d}\sigma_B}{\mathrm{d}\varphi_B}\right|_c\right)^{-1} \ . \qquad (18g)$$

The rate of change of σ_B with the CPC concentration φ_B is derived and substituted into Eqs (*18f*), (*18g*) in the Section 4.1.

Expansion of Eq. (*4b*) at the CP yields the critical binodal direction, i.e., the common slope of the binodal and spinodal at the CP in the isothermal multidimensional composition space,

$$\left.\frac{d\varphi_{Ki}}{d\varphi_{Kj}}\right|_c = \frac{\varphi_{Ki,c}\, r_{Ki}}{\varphi_{Kj,c}\, r_{Kj}}\ ,\qquad K = A, B\ , \tag{18h}$$

$$\left.\frac{d\varphi_{Bi}}{d\varphi_{Aj}}\right|_c = -\frac{\rho_{A,z}}{\rho_{B,z}}\frac{\varphi_{Bi,c}\, r_{Bi}}{\varphi_{Aj,c}\, r_{Aj}}\ .$$

As before in the case of ternary systems[8], it is somewhat surprising to see that for given chain-length distributions of A and B, the critical binodal direction is firmly fixed by the position alone of the CP in the composition space, and explicitly independent of interactions. Not so unexpected is the qualitative behavior indicated by the signs of the right-hand sides of Eqs (*18h*): a displacement along the critical binodal direction makes the concentrations of all components of, say, A vary in the same way (either all decrease or all increase), while those of B vary in the opposite direction.

4. MULTIPLE CRITICAL POINTS, STABILITY, AND THREE-PHASE REGIONS

Analogously to the case of solutions of polydisperse polymers[15–19], in polymer blends, too, the multiple CPs mark boundaries of "stability" for CPs and announce the proximity of a multi-phase region in the complete composition–temperature space. Since it is desirable to know the conditions under which such behavior can occur, the criteria for heterogeneous double CPs (HEDCPs) and triple CPs are derived below, and the implications for stability of CPs are discussed.

In all these considerations, various ratios of two consecutive averages for each polymer constituent turn out to play an important role. For the simplest case of polydisperse constituent, namely, a binary mixture of two polymer components P1 and P2 with chain lengths r_1, r_2 and weight fractions w_1 and $w_2 \equiv 1 - w_1$, the following facts may aid in choosing the parameters:

A) The ratio $Z_l(w_2) \equiv r_{z+l}/r_{z+l-1} = \zeta_{z+l}$ as function of w_2 reaches a maximum,

$$Z_{l,\max} = (\kappa^{1/2} + \kappa^{-1/2})^2/4\ , \tag{17b}$$

whose value depends only on the chain length ratio of the two components, $\kappa \equiv r_2/r_1$, but not on their absolute values or on the particular type of the ratio specified by the

subscript l. With increasing κ, all maximal ratios grow. Conversely, the chain-length ratio κ required for a desired maximum Z_{max} is

$$\kappa^* = 2Z_{max} - 1 + 2[Z_{max}(Z_{max} - 1)]^{1/2} \ . \tag{17c}$$

B) The weight fraction for the maximal Z_l, on the other hand, does depend on the index l (and on κ again), becoming smaller with growing l and κ,

$$w_{2,max} = (1 + \kappa^{l+1})^{-1} \ . \tag{17d}$$

The results are applicable even for negative l; e.g., the ratio r_w/r_n with $l = -1$ always peaks at $w_{2,max} = 1/2$.

C) Obviously, κ^* also represents the minimal chain-length ratio for which a desired ratio of consecutive averages is attainable at all. In that sense, $w_{2,max}$ of Eq. (*17d*) is a double root which splits into two single ones for chain-length ratios $\kappa > \kappa^*$. For instance, for a system with $r_1 = 10$, the maximal ratio $Z_{1,max} \equiv r_{z+1}/r_z = 2$ appears the first time for $\kappa \approx 5.8284$, i.e., for $r_2 \approx 58.284$, at $w_{2,max} \approx 0.02860$, in accord with the above equations. But when r_2 is increased to 60, i.e., by a mere 3%, the same ratio $Z_1 = 2$ now shows at two quite remote compositions, $w_2 \approx 0.0182$ and $w_2 \approx 0.0400$.

4.1. Heterogeneous Double Critical Points

A model phase diagram for a polymer blend with a three-phase region is displayed in Fig. 1. The system is a quaternary mixture, where each of the two constituents, A and B, consists of two species 1 and 2 with various chain lengths. While it is the simplest type possible, it already suffices to illustrate the essentials of phase relations in polydisperse blends.

The most striking feature is the bimodal character of the CPC (*1*), with an abrupt "break" at the three-phase point T in the "valley" where two of its stable branches intersect. Here the principal phase of concentration φ_T can be at equilibrium with either one of the incipient phases T^* and T^{**} located on the shadow curve (*2*). The metastable portions of the CPC extending from T downwards become unstable at the points of intersection with the spinodal (*3*) and, in general, continue towards the cusps C1 and C2, respectively, where they merge each with one end of the bottom unstable branch of the CPC. In the particular case depicted in Fig. 1, the system possesses a heterogeneous double critical point (HEDCP) overlapping with the cusp C2, hence the entire CPC section T-C$_2$ is metastable. While most obvious, the point T represents just one of a full spectrum of three-phase equilibria existing at various temperatures. For the chosen

polymers A and B, however, it is unique in being simultaneously a cloud-point at equilibrium with two different incipient phases; the rest of the three-phase region is buried under the stable CPC envelope, representing cases where the second and third phases are well developed.

The cusps C1 and C2 are singular, mathematically ill-behaved points where, drawn in g vs φ (or T vs φ) coordinates, the CPC "stops", "turns around" and continues with the same slope backwards in the opposite direction, while the parameters σ_K, ξ^2 and η^2 typically keep changing smoothly and monotonously. As a result, the derivatives of
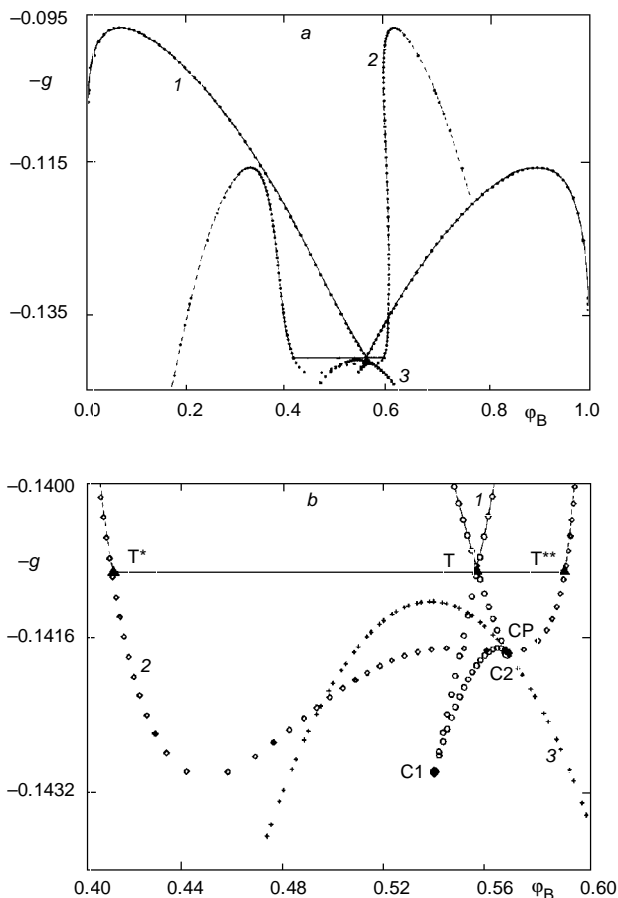
FIG. 1

Phase diagram for a three-phase quaternary system with $r_{A1} = r_{B1} = 10$, $r_{A2} = 150$, $r_{B2} = 300$, $w_{A2} = 4.65114 \cdot 10^{-2}$, and $w_{B2} = 7.85172 \cdot 10^{-3}$. Curves: *1* cloud-point curve (CPC), *2* shadow curve, *3* spinodal. Only stable portions of *1* and *2* are drawn by lines. The full-scale diagram from *a* is detailed in *b*: The CPC shows a three-phase point T and two cusps, C1 and C2, the latter one overlapping with the critical point CP; ▲—▲—▲ three-phase cloud-point equilibrium

some σ-based quantities along the CPC (e.g., $d\sigma_K/d\varphi_B$, $d\eta/dT$, etc.) here diverge. At the first sight, the classical rule about a cusp phase being conjugated with a spinodal point of the incipient phase, previously confirmed for binodals in ternary diagrams[15] and for CPCs in polydisperse polymer solutions[20], here seems to be broken: The shadow curve (*2*) minimum at $\varphi_{C1}^* \approx 0.448$, at equilibrium with the cusp C1, is clearly not intersected by the spinodal (*3*). This seeming discrepancy, however, is only one of many encountered in quasibinary CPC diagrams due to distortions in projecting spatial relations into the CPC plane. The spinodal drawn in Fig. 1 is entirely contained within the CPC plane, hence it is irrelevant for the position of the spinodal surface near the out-of-plane shadow-curve minimum. In fact, a simple calculation shows that at this minimum, the spinodal condition is met. A general proof that in polydisperse blends the incipient phase, coexisting with a cusp, belongs to the spinodal hypersurface is given in Appendix 2.

It is well known that in polydisperse polymer solutions, the CP can be located on any of the three CPC branches. For instance in a ternary system with $r_{A1} = r_{B1} = 1$, $r_{B2} = 25$, with the content w_{B2} of the high-molecular weight component B_2 growing, say, from $1 . 10^{-5}$ to 0.05, the CP moves from the high-φ_B stable CPC branch via the cusp of C1 type, the unstable branch T-C_2 and the other C2-type cusp, all the way to the low-φ_B stable branch[2,16]. A similar behavior is expected in the present case as the MMD's of polydisperse A and B are appropriately varied. Easily identifiable in this process is the moment when the CP passes through one of the cusps; here the CP becomes a heterogeneous double CP (HEDCP)[15,21] representing the overlap of two single CP's: one of the first kind, and the other of the second kind (cf. Korteweg[21]), or, in looser terms, of (meta)stable and unstable type, respectively. Thus the criterion for the appearance of an HEDCP is given by critical relations, Eqs (*18a*)–(*18d*), combined with the cusp condition

$$\lim_{\eta \to 0} \frac{d\varphi_B}{d\eta}\bigg|_{CPC} = 0 \ , \qquad (19a)$$

where the total derivative is taken along the CPC. A more useful form of this criterion in terms of partial derivatives of $\overline{F}$ function is derived in Appendix 1: from Eq. (*A1.3*) it is

$$\lim_{\eta \to 0} \left(\overline{F}_\eta + \overline{F}_\xi \frac{d\xi}{d\eta} \right) = 0 \ , \qquad (19b)$$

where the subscripts denote the partial derivatives [e.g., $\overline{F}_\eta \equiv (\partial \overline{F}/\partial \eta)_{\varphi, \xi}$]. The partial derivatives of $\overline{F}$ needed for Eq. (*19b*) are trivial, and the total derivative $d\xi/d\eta$ along the CPC is evaluated with the aid of $\overline{B}$ function (see Appendix 1). The final result for the HEDCP criterion is $S = 0$, where

$$S \equiv \rho_{A,z}(3r_{B,z} - r_{B,z+1}) + \rho_{B,z}(3r_{A,z} - r_{A,z+1}) \qquad (20a)$$

or, after dividing the equation by $\rho_{A,z}\rho_{B,z}$, even more simply $S' = 0$, where

$$S' \equiv S/(\rho_{A,z}\rho_{B,z}) \equiv \rho_{B,z}(3 - \zeta_{B,z+1}) + \rho_{A,z}(3 - \zeta_{A,z+1}) \quad . \qquad (20b)$$

These symmetrical forms of S are far more appealing than the earlier (albeit consistent) version

$$S \equiv 3r_z + 2\rho_z - r_{z+1} \qquad (20c)$$

derived for solutions of polydisperse polymers (i.e., for $r_A = 1$)[2,16,18]. If the criterial function S is negative, $S < 0$, the critical point is of the second kind in Korteweg's sense[21], i.e., the CPC in its neighborhood is thermodynamically unstable. (For the sake of brevity, the same stability qualifier is often employed for the CP itself, although, strictly speaking, one should use the Korteweg's term, or, relate the instability to the CPC.) A positive S, on the other hand, guarantees the CP's (meta)stability.

Interestingly, the slope of the CPC (Eq. (*18e*)) stays well defined, as demanded by the physics, even at an HEDCP where some other concentration derivatives diverge; as shown in Appendix 1, this is due to convenient cancellation of the two diverging terms containing $d\eta/d\varphi_B$ and $d\xi/d\varphi_B$. Also evaluated can now be the derivative $(d\sigma_B/d\varphi_B)_c$ required for the critical slope of the shadow curve, Eqs (*18f*, *18g*). From the definition of σ_B, Eq. (*12a*), it is apparent that this derivative is proportional to $(d\eta/d\varphi_B)_c$ discussed in Appendices 1 and 2. Thus, Eqs (*18f*, *18g*) ultimately yield for the shadow curve

$$2 \left.\frac{dg}{d\varphi_B^*}\right|_c = [(\zeta_{A,z})^{-1} - (\zeta_{B,z})^{-1}] \frac{S/(\varphi_B\rho_{A,q}\rho_{B,q})}{\varphi_A S - 4\rho_{A,z}r_{B,w}} \quad , \qquad (18i)$$

where S is defined by Eq. (*20a*). From here it is apparent that the shadow curve may show an extremum at the critical concentration for two reasons:

1. If the bracket of Eq. (*18i*) is zero, i.e., if the r_w/r_z ratio is the same for both polymers; in this case, also the CPC shows an extremum (cf. Eq. (*18e*)), and its common point with the shadow curve is a classical critical point.

2. If the stability criterion S for the principal phase is zero; that happens for a critical point located on the cusp of the CPC (cf. Fig. *1b*).

In other cases, the critical slope of the shadow curve is nonzero. Sometimes it may even diverge, with the shadow curve at the CP becoming vertical; this happens if the denominator of Eq. (*18i*) equals zero, i.e., if

$$\varphi_A S = 4\rho_{A,z} r_{B,w} \tag{18j}$$

or, with the aid of Eqs (*18b*) and (*20a*), if

$$\rho_{A,z}(3 - \zeta_{A,z+1}) + \rho_{B,z}(3 - \zeta_{B,z+1}) = 4(\rho_{A,q} + \rho_{B,q}) \ . \tag{18k}$$

It is immediately obvious from Eq. (*18j*) that the shadow curve cannot ever become vertical in the neighborhood of an unstable CP where $S < 0$; the CP has to be stable or metastable.

4.2. Stability

Two consequences of Eq. (*20b*) are immediately obvious: (i) If the ratios $\zeta_{A,z+1}$ and $\zeta_{B,z+1}$ for the two polymers A and B are low (specifically less than 3), the CP is stable or metastable. (ii) If both ratios are high (greater than 3), the CP is unstable.

The interesting case occurs if one ratio is low and the other is high, say, $\zeta_{A,z+1} < 3$, $\zeta_{B,z+1} > 3$; here the outcome may go either way. From Eq. (*20b*), the critical instability condition $S < 0$ then reads

$$\frac{\rho_{B,z}}{\rho_{A,z}} \frac{\zeta_{B,z+1} - 3}{3 - \zeta_{A,z+1}} > 1 \ . \tag{21a}$$

Thus, a B-polymer ratio $\zeta_{B,z+1} > \zeta^*$, where

$$\zeta^* \equiv 3 + 2(\rho_{A,z}/\rho_{B,z}) \ , \tag{21b}$$

guarantees the CP's instability regardless of $\zeta_{A,z+1}$, the ratio for the other polymer A (which obviously cannot be lower than 1, the value for a monodisperse A). The numerical value of ζ^* grows with decreasing chain length $r_{B,z}$ from the minimum of 3 (for a very high-molecular weight B, $\rho_{B,z} \to \infty$) to a hypothetical maximal value of $3 + 2\rho_{A,z}$ (corresponding to a somewhat unphysical situation of a monomeric B, $r_{B,z} = 1$, with its ratio $\zeta_{B,z+1} > 3$). These results are consistent with previous findings for ternary solutions[2,15,16]

(with $\rho_A = 1$) where the instability condition calls for the ratio $r_{B2}/r_{B1} > 15.645$ if $r_{B1} = 1$, or >9.899 if $r_{B1} \to \infty$.

The above considerations clearly show that instability of CPs in quasibinary polymer blends is far from being a common phenomenon; just like in the case of solutions of polydisperse polymers, a high ratio $\zeta_{B,z+1}$ for at least one polymer is necessary. In fact, if anything, the tendency towards instability at constant $\zeta_{A,z+1}$ and $\rho_{B,z}$ decreases as the "solvent" A becomes polymeric, since higher ratios $\zeta_{B,z+1}$ are required for it (cf. Eq. (*21a*)).

Equation (*21a*) also indicates that the $\zeta_{K,z+1}$ ratios of both polymers show synergism in achieving instability: For instance, at constant $r_{A,z}$ and $r_{B,z}$, the demand for high ratio $\zeta_{B,z+1}$ of the B distribution is alleviated by an increase in the ratio $\zeta_{A,z+1}$ of the A distribution.

Perhaps it should be pointed out that in developing the present picture of phase behavior, the illustrations in papers of one of us (K. S.) were not always accurate:

a) The ranges of the cloud-point curve stability schematically shown in Fig. 1 of refs[22,23] from early seventies are not general. A CPC cusp acts as a separator of unstable and metastable portions of the CPC only if it is also occupied by a CP, i.e., if the system happens to possess an HEDCP. In general, however, cusps will stay unstable, and the boundary between unstable and metastable portions of the CPC is shifted towards the three-phase point T. The boundary can be located by using the spinodal condition[1] as the stability criterion for off-critical phases.

b) The pointed extrema of the shadow curve drawn in Fig. 1 of ref.[22] are only schematic; as shown later[20], the extrema should be perfectly normal, of round shape and zero slope. Since they represent projections of incipient phases conjugated with the CPC's cusps, however, they have to belong to the spinodal hypersurface[15,20] (although they may not be located on the spinodal often drawn for the CPC's composition plane (cf. Fig. 1*b*)). Thus, noncritical extrema do act as separators of unstable and (meta)stable portions of the shadow curve, even in polydisperse blends. The uneasiness intuitively felt due to possibly having, e.g., an unstable point of the CPC at equilibrium with a (meta)stable incipient phase of the shadow curve is uncalled for. Such a combination is feasible since the equilibrium merely requires equality of chemical potentials at two distant phase compositions, whereas the phase stability is the matter of the local rate of change of chemical potentials with composition (that may well be opposite at two distant points sharing the same chemical potentials). In fact, such cases of a metastable phase equilibrated with an unstable phase may occur even in binary systems when the interaction function is concentration dependent (see, e.g., Fig. 9*a* of ref.[24]).

c) Also, the point of intersection of the two stable CPC branches was at first referred to as the "triple" point[2]. On second thought, it was realized that this was not a suitable term, particularly because of possible confusion with an entirely different "triple critical" point. Hence, a more appropriate term "three-phase" point was later introduced (cf. a note on p. 1952, ref.[16]).

4.3. Triple Critical Points

In ternary systems the role of HEDCPs and triple CPs is very unique. For instance, in the particular system mentioned in Section 4.1. ($r_{A1} = 1$; $r_{B1} = 1$, $r_{B2} = 25$), the two HEDCPs occupy a local maximum (at $w_{B2} \approx 4.2 \cdot 10^{-4}$) and minimum (at $w_{B2} \approx 9.4 \cdot 10^{-3}$) of the critical line, and are embedded in the three-phase region. With decreasing chain length r_{B2}, both the interval between the two HEDCPs and the size of the three-phase region shrink, until they disappear entirely in a triple CP at $w_{B2} \approx 4.95 \; 10^{-3}$ as r_{B2} reaches the value of $r^* \approx 15.645$. Such a case marks transition between systems (with $r_{B2} < r^*$) whose CPC is smooth for all compositions w_{B2}, and those (with $r_{B2} > r^*$) whose CPC, in a certain range of w_{B2}, consists of three branches, and carries a three-phase point and two cusps. The physical interpretation is here so simple since, at constant r_A and r_{B1}, this is essentially a one-degree-of-freedom problem where only r_{B2} is allowed to vary.

It is obvious that the situation will be much more complex in polydisperse polymer blends whose distributions can be varied in many different dimensions. Common to all such cases, however, should be the fact that the triple CP arises, as before, by merging of two HEDCPs; hence it requires that, in addition to the HEDCP condition (*19a*), also the second total derivative of φ_B along the CPC be zero

$$\lim_{\eta \to 0} \frac{d^2 \varphi_B}{d\eta^2}\bigg|_{CPC} = 0 \qquad (22a)$$

or, alternatively,

$$\lim_{\eta \to 0} \frac{d^2 F}{d\eta^2}\bigg|_{\varphi_B} = \lim_{\eta \to 0}\left[F_{\eta\eta} + 2F_{\eta\xi}\frac{d\xi}{d\eta} + F_{\xi\xi}\left(\frac{d\xi}{d\eta}\right)^2 + F_\xi\frac{d^2\xi}{d\eta^2}\right] = 0 \; . \qquad (22b)$$

Not surprisingly, the criteria (*19b*) and (*22b*) are formally identical to the corresponding conditions for ternary systems, Eq. (*18*) and (*22*) of ref.[12], only the cloud-point function F employed here is different.

The additional condition (*22b*) for the triple critical point can be simplified by using the HEDCP criterion, and recast again in terms of chain-length averages as a symmetric compact relation

$$T_{CP} \equiv r_{A,z} r_{B,z+1}(5r_{B,z+1} - 3r_{B,z+2}) - r_{B,z} r_{A,z+1}(5r_{A,z+1} - 3r_{A,z+2}) = 0 \; . \qquad (23a)$$

For a polydisperse polymer solution ($r_A = 1$) the criterion (*23a*), combined with the condition $S = 0$ (cf. Eq. (*20c*)), correctly reduces to the previously reported, less attractive asymmetric version[2,18]

$$T_{CP} \equiv 15r_z^2 + 20r_z\rho_z + 6r_z - r_{z+1}r_{z+2} = 0 \ . \tag{23b}$$

From Eq. (*23a*) it is apparent that of primary importance for the existence of a triple CP in blends are the ratios of even higher chain-length averages, $\zeta_{K,z+2} \equiv r_{K,z+2}/r_{K,z+1}$. For instance, the CPC will possess a triple CP independently of their averages $r_{A,z}$ and $r_{B,z}$ if, for both polymers, these ratios assume the value of 5/3 ($= \zeta_{A,z+2} = \zeta_{B,z+2}$), and if $\zeta_{A,z+1} = \zeta_{B,z+1} = 3$ to satisfy the condition $S = 0$ for an HEDCP (cf. Eq. (*20a*)).

Interesting is the correlation between effects of the two $\zeta_{K,z+2}$'s, clearly seen from the rearranged form of Eq. (*23a*)

$$\frac{\zeta_{B,z+1}}{\zeta_{A,z+1}} \frac{r_{B,z+1}}{r_{A,z+1}} \frac{5 - 3\zeta_{B,z+2}}{5 - 3\zeta_{A,z+2}} = 1 \ . \tag{23c}$$

A triple CP cannot appear if $\zeta_{B,z+2} > 5/3$ and $\zeta_{A,z+2} < 5/3$, or vice versa; in certain sense one might say that it requires both polymers A and B to be "comparable" in their ratios r_{z+2}/r_{z+1} (either both should be <5/3, or both should be >5/3). This demand for "likeness" is also revealed by the behavior of systems which happen to possess a triple CP already: In order to keep it during perturbation of the MMDs of A and B, an increase in, say, $\zeta_{A,z+2}$ ratio for A (at constant r_z's and r_{z+1}'s) necessitates another increase in $\zeta_{B,z+2}$ for the other polymer B. Even stronger argument for the above claim is offered by the ultimate case of "likeness" when both distributions of A and B are identical, i.e., $w_A(r) \equiv w_B(r)$; then the condition $T_{CP} = 0$ is satisfied automatically, and the existence of a triple CP symmetrically located at $\varphi_{A,c} = \varphi_{B,c} = 1/2$ merely requires matching the HEDCP criterion $S = 0$. Thus the joint effect of the two $\zeta_{K,z+2}$'s on the triple CP criterion turns out to be just the opposite from the synergetic action of the two $\zeta_{K,z+1}$'s on the HEDCP condition. This difference in behavior originates in the signs of the two symmetrical terms in the respective criteria: they are the same in Eq. (*20a*), but they are opposite in Eq. (*23a*).

If A is monodisperse, the triple CP criterion (*23a*), combined with the HEDCP condition $S = 0$ (see Eq. (*20a*)), yields a simple explicit formula for the triple-CP ratio $\zeta_{B,z+2}$ as a function of only the chain-length ratio $r_{B,z}/r_A$

$$3\zeta_{B,z+2} = 5 - \frac{2}{(2 + 3\rho_{B,z}/\rho_A)^2} \ . \tag{23d}$$

Equation (*23d*) reveals that the effect of moving from a monomeric to polymeric solvent A on the ratio $\zeta_{B,z+2}$ required for a triple CP is very mild, albeit opposite to that observed for HEDCP alone. The ratio stays practically constant at $\zeta_{B,z+2} \approx 5/3$ as long as B is much longer in chain length than A, $r_{B,z} \gg r_A$. Letting the monodisperse solvent A grow in molecular size makes the right-hand side of Eq. (*23d*) greater, thereby somewhat reducing the required magnitude of $\zeta_{B,z+2}$. The effect, however, is very small: When A and B become equal in size ($r_A = r_{B,z}$), the needed $\zeta_{B,z+2}$ is still 1.64, and even in the other limit for $r_A/r_{B,z} \to \infty$, $\zeta_{B,z+2}$ should equal 1.5.

The validity of Eq. (*23d*) is supported by two well known triple-CP ternary systems[15,16]: (i) For the one mentioned at the beginning of this section, with $r_A = 1$, $r_{B1} = 1$, $r_{B2} = 15.645$ and $w_{B2} \approx 4.95 \cdot 10^{-3}$, the ratio is $\zeta_{B,z+2} \approx 1.650$, whether computed from the mixture composition or from Eq. (*23d*). (ii) If the molecular weight of polymer B becomes very high while that of A stays finite, i.e., with $r_A = 1$ and $r_{Bi} \to \infty$, the required ratio of the two B fractions drops to $r_{B2}/r_{B1} = 9.899$, and the B-composition of the triple-CP system is $w_{B2} \approx 0.01010$. Here again, both methods of calculation yield the same ratio $\zeta_{B,z+2}$ 1.6667.

5. EXAMPLES

First, several computed phase diagrams will be shown that confirm various quantitative criteria derived above. Then some model calculations of more general character will be presented.

Figure 2 displays phase diagram for a symmetrical polymer blend with $\zeta_{A,z+1} = \zeta_{B,z+1} = 3$ that should possess a triple CP (cf. Eqs (*20b*) and (*23c*)); specifically, both polymers A and B here consist of two components with $r_{A1} = r_{B1} = 10$, $r_{A2} = r_{B2} = 150$, and $w_{A2} = $
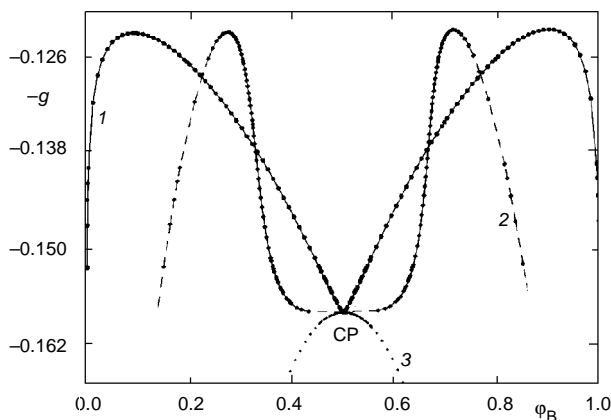

FIG. 2

Phase diagram for a symmetrical quaternary blend with a triple CP, with parameters $r_{A1} = r_{B1} = 10$, $r_{A2} = r_{B2} = 150$, $w_{A2} = w_{B2} = 1.875623 \cdot 10^{-2}$. Notation is the same as in Fig. 1

$w_{B2} = w''_{2,S} = 1.87562 \cdot 10^{-2}$. Quite surprising is the deep valley on the bimodal CPC, resembling diagrams with eutectic points, in stark contrast to typical polymer solution CPCs that were flat in the vicinity of a triple CP (ref.[18]). Unlike in a real eutectic, however, the two sloping portions of the CPC do not intersect yet. As before, the CPC at $\varphi_B = 1/2$ is just on the verge from being smooth and round (for $w_{A2} = w_{B2} > w''_{2,S}$, where $S > 0$) to displaying an intersection of two CPC branches, with the familiar non-stable "triangle" and two cusps below the stable CPC envelope (for $w_{A2} = w_{B2} < w''_{2,S}$, where $S < 0$). Examples for both cases are detailed in Figs 3*a* and 3*b*. At first sight it might be
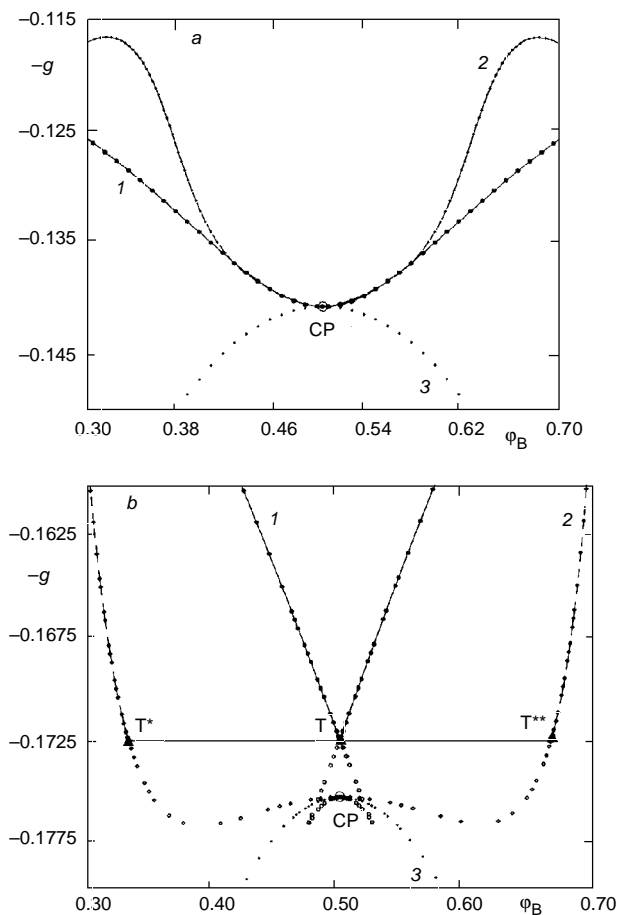
FIG. 3

Two magnified midsections of phase diagrams for systems derived from that of Fig. 2 by perturbing the compositions of A and B. Notation is the same as in Fig. 1. *a* for $w_{A2} = w_{B2} = 0.03$, $S > 0$ and the CPC becomes smooth; *b* for $w_{A2} = w_{B2} = 0.01$, $S < 0$ and a three-phase point and two cusps appear on the CPC

objected that no splitting of the triple CP into two HEDCPs is apparent here since in symmetrical blends, the lone CP always stays in the middle at $\varphi_{B,c} = 1/2$. However if the symmetry condition is rescinded, the transition from Fig. 2 to Fig. 3*b* can also be made by many other pathways where the HEDCP will show up either on the left or on the right cusp; hence, in that sense our original thesis is justified.

The above statement about the behavior of systems with $w_{A2} = w_{B2} < w''_{2,S}$ is correct only up to a point. As explained at the beginning of Section 4, the function $\zeta_{z+1}(w_2)$ possesses a maximum beyond which it starts descending, capable of assuming the above value of $\zeta_{z+1} = 3$ again. Indeed, such a second root of the equation $S = 0$ is found at $w_{A2} = w_{B2} = w'_{2,S} \approx 1.03233 \cdot 10^{-3}$ where the CPC displays a triple CP again. Understandably, for $w_{A2} = w_{B2} < w'_{2,S}$ the CPC is again stable and smooth in all of its length.

Although the triple CP criterion $T_{CP} = 0$ is trivially satisfied for any symmetrical blend, a "stronger" zero results if for both polymers also $\zeta_{z+2} = 5/3$ (cf. Eq. (*23a*)). Keeping r_{A1} and r_{B1} fixed at 10 and both ratios ζ_{z+1} at 3, that happens for $r_{A2} = r_{B2} \approx 98.9899$ at $w_{A2} = w_{B2} = w_{2,S} \approx 0.010101$. These values are familiar: the same w_{B2} and the same component ratio $r_{B2}/r_{B1} \approx 9.89899$ characterize the triple CP if A is a monomeric solvent and $r_{Bi} \to \infty$, as shown long ago by Tompa[15]. Furthermore, the genesis of the triple CP is here the same as well: it arises as a double root of the condition $S(w_2) = 0$, i.e., the criterial function $S(w_2)$ of Eq. (*20a*) here displays a minimum just touching on the axis w_2 at $w_2 = w_{2,S}$. A small perturbation of w_2 in either direction from $w_{2,S}$ results in the CPC becoming smooth and stable in its entire length. The phase diagram looks similar to that of Fig. 2.

Example of an asymmetric blend with an HEDCP was shown in Fig. 1; it contains no new features relative to the diagrams of polydisperse polymer solutions with an HEDCP, except for the profound rift in the critical region. Perhaps worth noting are dependences of number, weight, and z-averages of polymers A and B separated into the incipient phase, plotted as functions of the principal phase concentration φ_B and displayed in Figs 4*a* and *b*. The results pointedly illustrate the strong, almost exclusive preference of low-molecular weight component of one polymer to penetrate into the phase rich in the other[4,25]. For instance in the case of blends poor in B (say, with $\varphi_B < 0.4$), the B-rich incipient phase appearing at the cloud point contains practically only the lower A-component but very little of the higher one, as indicated by all three plotted averages, $r^*_{A,n}$, $r^*_{A,w}$ and $r^*_{A,z}$, being about 10 (see Fig. 4*a*). On the other hand, the rich-in-A incipient phase separated from a rich-in-B blend contains predominantly the higher A component, squeezed out of the B-rich environment. This is apparent, for instance, from high values of $r^*_{A,z}$ shown for blends rich in B (say, with $\varphi_B > 0.6$), compared to the original value in pure A, $r_{A,z} \approx 69.15$. The described behavior is even more conspicous for polymer B with higher polydispersity (see Fig. 4*b*).

For an asymmetric blend with preselected chain lengths $r_{A1} = r_{B1} = 10$, $r_{A2} = 150$ and $r_{B2} = 300$, the triple CP conditions $T_{CP} = 0$ and $S = 0$ leave no more degrees of freedom

in A and B compositions (although there may be more than one solution). A triple CP is found for $w_{A2} \approx 0.4969377$ and $w_{B2} \approx 1.672973 \cdot 10^{-3}$, with coordinates $\varphi_B \approx 0.757374$ and $g \approx 8.88615 \cdot 10^{-2}$. The phase diagram for this case is shown in Fig. 5. Its CPC is still smooth, displaying a strong depression. Again, appropriate perturbations in composition would create systems with a three-phase region. For instance, for $w_{A2} = 0.25$ and $w_{B2} \approx 2.97644 \cdot 10^{-3}$ an HEDCP is positioned on the right cusp, whereas for $w_{A2} = 0.25$ and $w_{B2} \approx 8.8707 \cdot 10^{-4}$ an HEDCP occupies the left cusp.
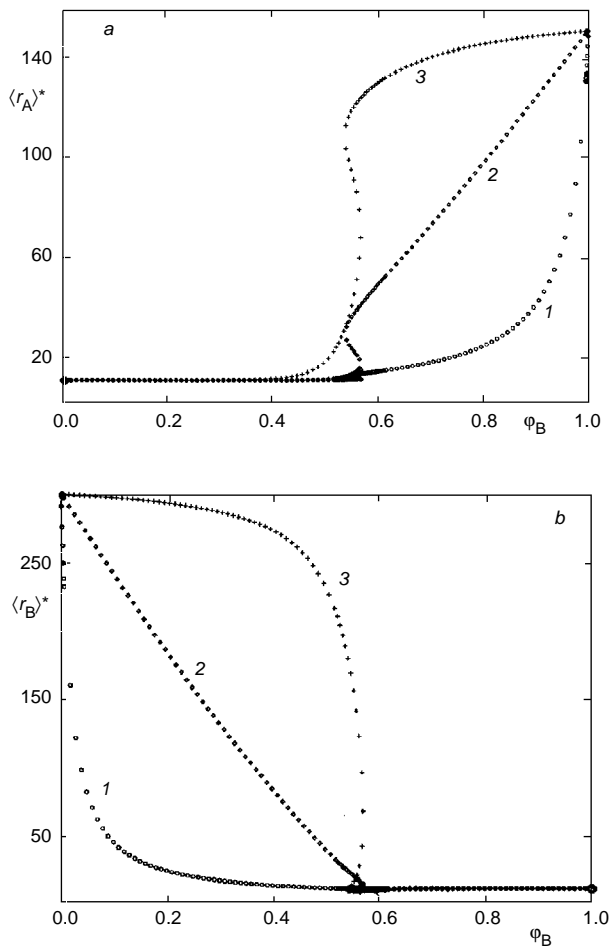
FIG. 4

Average chain lengths of the polymer contained in the incipient phase appearing at the cloud point of solutions of composition φ_B for the system of Fig. 1: *1* number average, *2* weight average, *3* z-average. *a* Polymer A, *b* polymer B

Finally, we would like to check the condition derived for the critical slope of the shadow curve, Eq. (*18i*). An illustrative way of doing that is to compute the phase diagram for a system compatible with Eq. (*18j*), derived from Eq. (*18i*) for the case of vertical shadow curve. For this demonstration, the chain lengths of the four components
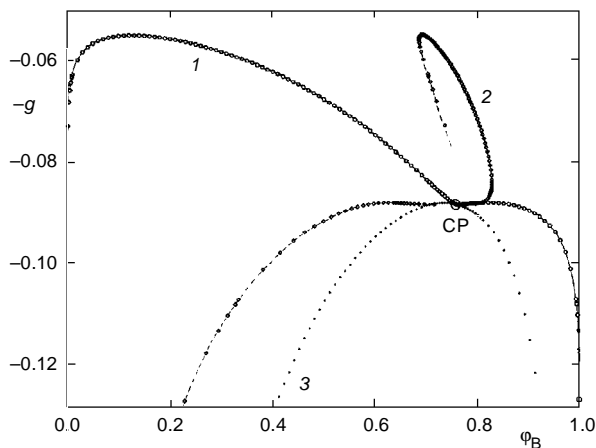

FIG. 5

Phase diagram for an asymmetric blend with components' chain lengths identical to those of Fig. 1, and the compositions $w_{A2} \approx 0.496938$ and $w_{B2} \approx 1.67297 \cdot 10^{-3}$ that characterize a blend with a triple critical point
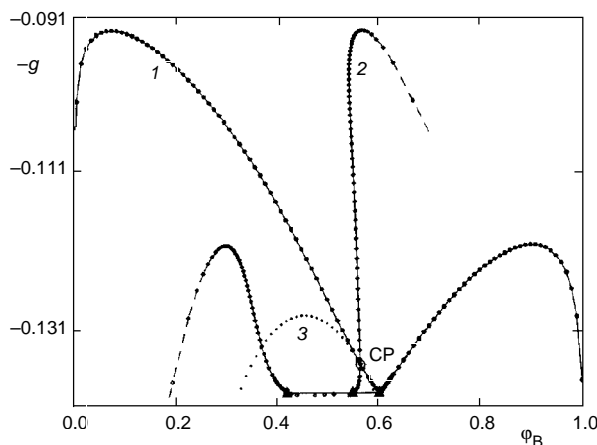

FIG. 6

Phase diagram for an asymmetric blend of the same chain-length characteristics as employed in Fig. 1, with its composition chosen so as to make its shadow curve vertical at the critical point. The constituents' compositions $w_{A2} = 0.02$ and $w_{B2} \approx 3.10185 \cdot 10^{-2}$ satisfy Eq. (*18j*)

are left unchanged, i.e., $r_{A1} = r_{B1} = 10$, $r_{A2} = 150$ and $r_{B2} = 300$. For the chosen composition of A, $w_{A2} = 0.02$, the composition of B has to be taken as $w_{B2} \approx 3.10185 \cdot 10^{-2}$ to satisfy Eq. (*18j*); the CP is then at $\varphi_B \approx 0.559466$ and $g \approx 0.135720$, with a positive stability parameter $S \approx 1\ 128.5$ (cf. Eq. (*20a*)). The numerically computed diagram for this case in Fig. 6 indeed shows a shadow curve that becomes vertical in the neighborhood of the critical point; it also displays a three-phase region.

In another set of calculations on four-component blends, we examine the effect of varying the chain-length ratios $\zeta_w \equiv r_w/r_n$ and $\zeta_z \equiv r_z/r_w$ at constant weight-average r_w.

Figure 7 shows a symmetrical quasi-binary (QB) phase diagram calculated for $r_{K,w} = 1\ 000$, where K = A, B. Curve *1*, added for comparison, refers to a strictly binary blend with $r_A = r_B = 1\ 000$, whereas the curves *2* and *3* have common $\zeta_{K,w} = 2$ but differ in their $\zeta_{K,z}$ (which is 1.5 for *2* and 2.5 for *3*). The CPCs all become very soon (say for $g > 0.005$) indistinguishable from pure-A and -B axes, for polydisperse blends even more so than for the binary mixture. This behavior has often been incorrectly interpreted as a proof of almost perfect immiscibility for most of the polymers. In fact it merely means that, when increasing the g parameter, the incipient phase separation starts very early, even for an almost pure polymer containing only traces of the other polymer. Moreover, note
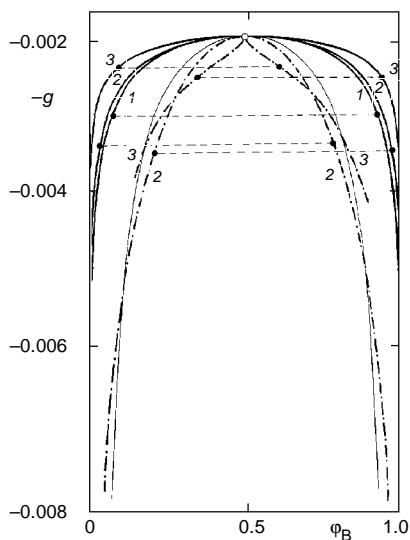
FIG. 7

Quasi-binary (QB) phase diagram calculated for symmetrical blends, $r_{A,w} = r_{B,w} = 1\ 000$: CPC (heavy solid line), shadow curve (dot and dash line), spinodal (light solid line), horizontal tie-lines (dashed lines); *1* single-component polymers A and B, *2* and *3* $\zeta_{A,w} = \zeta_{B,w} = 2$; *2* $\zeta_{A,z} = \zeta_{B,z} = 1.5$; *3* $\zeta_{A,z} = \zeta_{B,z} = 2.5$
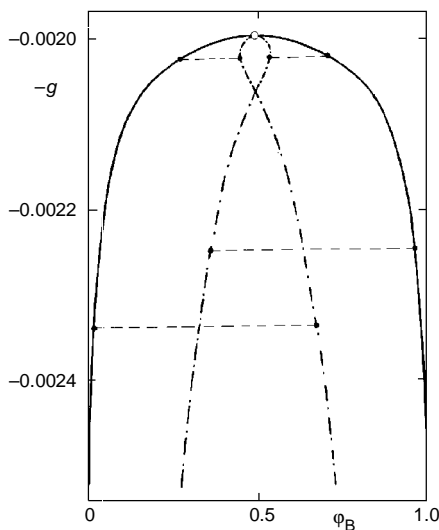
FIG. 8

The same as Fig. 7 except for $\zeta_{A,z} = \zeta_{B,z} = 4.0$

that the CPC is useless as a measure of mutual solubility unless the system is strictly binary. In practice one has a multicomponent blend in which the shadow curve may deviate markedly from the CPC, indicating sizeable mutual solubility in the incipient phase up to high values of g. In fact, shadow curves do not merge into the axes representing pure constituents until the system is cooled down close to 0 K ($g \to \infty$). Strictly speaking, the same is true for CPC's but for all practical purposes, these curves are indistinguishable from the axis already at g values not far above the critical value.

The cusp seemingly formed by the shadow curve *3* at the CP is not real, and the distortion can be easily understood: In strictly binary blends, in which A and B are both monodisperse, the CPC and shadow curve coincide in a single coexistence curve (binodal) contained in the $g(\varphi_B)$ plane. With growing polydispersity index ζ_w the shadow curve, anchored at all times in the plane by the CP, starts pivoting around its anchor and moving more and more out of the CPC plane, until it runs "perpendicularly" to it; then the shadow curve projects onto the CPC plane as a vertical cusp touching on the CP. It
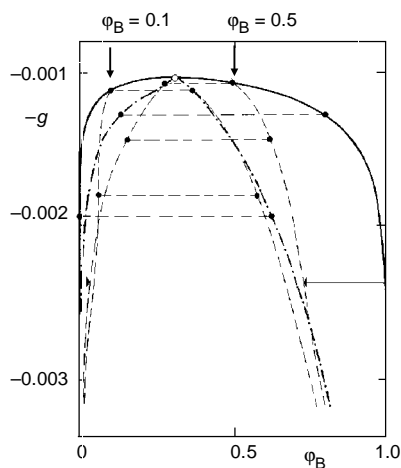

F$_{IG}$. 9

QB phase diagram for an asymmetric blend, $r_{A,w} = 1\ 000$, $r_{B,w} = 5\ 000$, $\zeta_{A,w} = \zeta_{B,w} = 2$, $\zeta_{A,z} = \zeta_{B,z} = 2$. Line notation the same as in Fig. 7, with additional coexistence curves (– – –) shown for φ_B 0.1 and 0.5. Horizontal arrows indicate thermodynamic aging at $\varphi_B = 0.5$ and $g \approx 2.375 \cdot 10^{-3}$
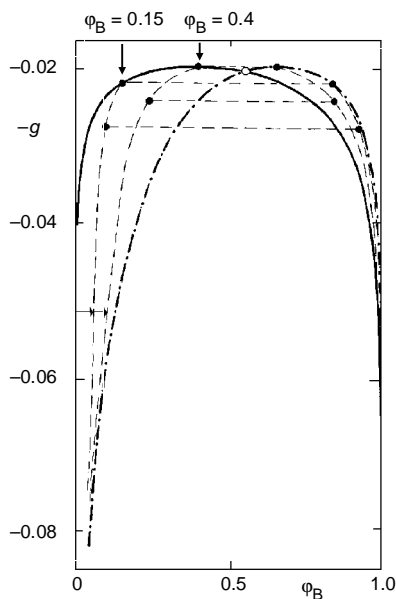
F$_{IG}$. 10

QB phase diagram for a blend symmetrical in r_w (= 100). Polymer A: monodisperse; polymer B: $\zeta_{B,w} = 2$, $\zeta_{B,z} = 1.5$. Symbols the same as in Fig. 9

can be shown that for symmetrical blends, like those of Fig. 7, this occurs when their r_z reaches the value $r_z^\#$, where

$$r_z^\# = (4r_w + r_{z+1})/3 \ . \tag{24}$$

It so happens that the curve *3* in Fig. 7 almost matches this condition; its r_z deviates from $r_z^\#$ of Eq. (*24*) by a mere $\approx 1.3\%$. When r_z grows further above $r_z^\#$, the shadow curve in the multidimensional composition space continues pivoting around the CP, and an apparent loop with a point of self-intersection arises on its projected $g(\varphi_B^*)$ image (see Fig. 8). As follows from the above, in symmetrical blends such a point can appear only if $r_z > r_z^\#$, and it can be pinpointed as an equilibrium where the computed noncritical incipient phase concentration φ_B^* equals 1/2.

Although the location of the shadow curves already suggests sizeable mutual solubility, we need coexistence curves to judge whether fully phase-separated blends should be expected to exhibit a similar phenomenon. Figure 9 represents a non-symmetric blend and shows coexistence curves in addition to cloud point and shadow curves. For instance, a 50/50 blend ($\varphi_B = 0.5$), if completely phase separated, would follow its dashed curves and would, in equilibrium, not be immiscible unless g becomes very high (and T very low). The phase concentrated in polymer B contains sizeable amounts of the low-molar mass components in polymer A. The reverse is true for the other phase. There is no true immiscibility though a measurement of the CPC would suggest such behavior at $g > 0.0025$. Analogous behavior must be expected with blends symmetrical in r_w.

These findings indicate that the concept of almost absolute immiscibility in some polydisperse polymer blends has to be questioned. Blending produces a more or less
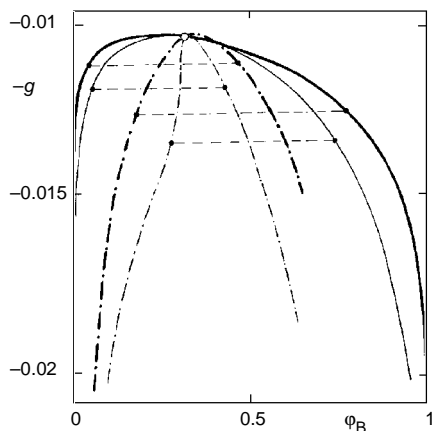

Fig. 11
QB phase diagram for two asymmetric blends, $r_{A,w} = 100$, $r_{B,w} = 500$, $\zeta_{A,w} = 2$, $\zeta_{B,w} = 3$, $\zeta_{A,z} = 1.75$, $\zeta_{B,z} = 2$. Line types the same as in Fig. 7: polymers A and B are binary mixtures (light lines), polymers A and B with continuous molar-mass distributions (heavy lines)

finely dispersed two-phase system in which the two phases will initially consist of almost pure polymers A and B. However slowly, the system is forced toward mutual solubility to some degree. This process of thermodynamic aging cannot be stopped unless special measures are taken. If one or both phases vitrify upon cooling the aging process will be stopped, to be revived again when reprocessing the blend. An effective means of stopping thermodynamic aging is provided by cross-linking of one or both phases.

Calculation of the quasi-binary phase diagram for a blend consisting of a monodisperse component A and a polydisperse polymer B corroborates the remarks on fractionation made above. Figure 10 demonstrates that in such cases thermodynamic aging must be expected to occur predominantly on the left, A-rich, side of the diagram.

Finally, Fig. 11 exemplifies that the type of molar-mass distribution, at identical r_w, ζ_w and ζ_z, influences the phase diagram markedly. We compare blends consisting of two binary polymers (light curves) and of two polymers with continuous distributions of Schulz–Zimm type (heavy curves). This result is consistent with similar conclusions on polymer solutions, reported previously[26].

APPENDIX 1

Total derivatives along the CPC can be evaluated from the differentials of cloud-point functions. Particularly advantageous are the functions $\overline{F}$ and $\overline{B}$ (as opposed to $\overline{G}$) since they contain no interaction parameter g, hence they do not depend explicitly on temperature. Choosing ξ, η and φ_B as independent variables, the total differentials are

$$d\overline{F} = \overline{F}_\xi d\xi + \overline{F}_\eta d\eta + \overline{F}_\varphi d\varphi_B = 0 \quad , \tag{A1.1}$$

$$d\overline{B} = \overline{B}_\xi d\xi + \overline{B}_\eta d\eta + \overline{B}_\varphi d\varphi_B = 0 \quad . \tag{A1.2}$$

With no loss of generality, $d\varphi_B$ can be eliminated by combining Eqs (A1.1) and (A1.2). For instance, from Eq. (A1.1) one has

$$\frac{d\varphi_B}{d\eta} = -\left(\overline{F}_\xi \frac{d\xi}{d\eta} + \overline{F}_\eta\right)\bigg/\overline{F}_\varphi \tag{A1.3}$$

which, substituted into Eq. (A1.2), leads to the derivative

$$\frac{d\xi}{d\eta} = \frac{\overline{B}_\eta \overline{F}_\varphi - \overline{B}_\varphi \overline{F}_\eta}{\overline{B}_\varphi \overline{F}_\xi - \overline{B}_\xi \overline{F}_\varphi} \quad . \tag{A1.4}$$

Equation (*A1.3*) confirms that the HEDCP conditions (*19a*) and (*19b*) are indeed consistent.

The slope of the CPC is derived from the function $\overline{G}$ for which, analogously to Eqs (*A1.1*) and (*A1.2*), one can write

$$\frac{d\overline{G}}{d\varphi_B} = \overline{G}_g \frac{dg}{d\varphi_B} + \overline{G}_\varphi + \overline{G}_\eta \frac{d\eta}{d\varphi_B} + \overline{G}_\xi \frac{d\xi}{d\varphi_B} = 0 \quad . \tag{A1.5}$$

With $d\xi/d\varphi_B$ expressed from Eq. (*A1.1*)

$$\frac{d\xi}{d\varphi_B} = -\frac{\overline{F}_\varphi + \overline{F}_\eta (d\eta/d\varphi_B)}{\overline{F}_\xi} \tag{A1.6}$$

and $d\eta/d\varphi_B$ available from Eq. (*A1.3*), the relation for the CPC slope, $dg/d\varphi_B$, can be obtained from Eq. (*A1.5*).

Equations (*A1.1*)–(*A1.6*) are entirely general, and have to be satisfied at any point of the CPC. Their specific forms for critical state are obtained by employing the expanded forms (*13*)–(*15*) for $\overline{F}$, $\overline{G}$, and $\overline{B}$, and taking the limit for $\eta \rightarrow 0$. Equation (*A1.4*), combined with Eq. (*19b*), then yields the practical form of the HEDCP criterion, Eq. (*20a*); in addition, its total derivative relative to η yields the second derivative $d^2\xi/d\eta^2$ required in Eq. (*22b*) to provide the practical form (*23a*) of the triple CP criterion. Also, the derivation of the expression (*18e*) for the critical CPC slope, $(dg/d\varphi_B)_c$, from the limiting forms of Eqs (*A1.3*), (*A1.5*) and (*A1.6*) should be trivial.

The presence of the terms $d\eta/d\varphi_B$ and $d\xi/d\varphi_B$ in Eq. (*A1.5*) might raise concern about the soundness of these formulas around HEDCPs where these derivatives diverge. Fortunately, it turns out that with $d\xi/d\varphi_B$ of Eq. (*A1.6*) substituted into Eq. (*A1.5*), the combined coefficient of the ill-behaved term $d\eta/d\varphi_B$ becomes zero and in effect removes the divergence, yielding the result (*18e*) for the critical CPC slope, applicable even at an HEDCP.

APPENDIX 2

At a cusp of the CPC, $d\varphi_B/d\eta$ of Eq. (*A1.3*) has to be zero. After substituting $d\xi/d\eta$ from Eq. (*A1.4*) into Eq. (*A1.3*), its right-hand side can be simplified and the above cusp criterion written as

$$B_\eta F_\xi - B_\xi F_\eta = 0 \quad . \tag{A2.1}$$

After substituting the derivatives from Eqs (*5*) and (*8a*), and employing Eq. (*6a*) to introduce the interaction parameter *g*, the condition (*A2.1*) takes the form

$$2g - (\varphi_A^* r_{A,w}^*)^{-1} - (\varphi_B^* r_{B,w}^*)^{-1} = 0 \qquad (A2.2)$$

which is recognized as the equation of the spinodal[1] written for the conjugate phase. Hence, the incipient phase coexisting with a CPC's cusp point belongs to the spinodal hypersurface.

REFERENCES

1. Koningsveld R., Kleintjens L. A., Schoffeleers H. M.: Pure Appl. Chem. *39*, 1 (1974).
2. Solc K.: Macromolecules *3*, 665 (1970).
3. *Polymer Software*. BIOSYM Technologies, Inc., San Diego, CA 92121 (____).
4. Koningsveld R., Solc K., MacKnight W. J.: Macromolecules *26*, 6676 (1993).
5. Flory P. J.: *Principles of Polymer Chemistry*, Chap. 13. Cornell University Press, Ithaca, N.Y. 1953.
6. Huang Y.-H., Solc K.: ACS Polym. Prepr. (Am. Chem. Soc., Div. Polym. Chem.) *30*, No. 2, 112 (1989).
7. Solc K.: Makromol. Chem., Macromol. Symp. 7*0/71*, 93 (1993).
8. Solc K.: Macromolecules *19*, 1166 (1986).
9. Koningsveld R., Staverman A. J.: Kolloid.-Z. Z. Polym. *218*, 114 (1967).
10. Rehage G., Moller D., Ernst O.: Makromol. Chem. *88*, 232 (1965).
11. Rehage G., Moller D.: J. Polym. Sci., C *16*, 1787 (1967).
12. Solc K.: Macromolecules *20*, 2506 (1987).
13. Koningsveld R., Chermin H. A. G., Gordon M.: Proc. R. Soc. London A *319*, 331 (1970).
14. Stockmayer W. H.: J. Chem. Phys. *17*, 588 (1949).
15. Tompa H.: Trans. Faraday Soc. *45*, 1142 (1949).
16. Solc K.: J. Polym. Sci., Polym. Phys. Ed. *20*, 1947 (1982).
17. Solc K.: Macromolecules *16*, 236 (1983).
18. Solc K., Kleintjens L. A., Koningsveld R.: Macromolecules *17*, 573 (1984).
19. Solc K., Battjes K.: Macromolecules *18*, 220 (1985).
20. Solc K.: Macromolecules *10*, 1101 (1977).
21. Korteweg D. J.: Sitzungsber. Kais. Akad. Wiss., Math.-Naturwiss. Klasse *98* (2 Abt. A), 1154 (1889).
22. Solc K.: J. Polym. Sci., Polym. Phys. Ed. *12*, 555 (1974).
23. Solc K.: Macromolecules *8*, 819 (1975).
24. Solc K., Dusek K., Koningsveld R., Berghmans H.: Collect. Czech. Chem. Commun. *60*, 1661 (1995).
25. Beaucage G., Stein R. S., Koningsveld R.: Macromolecules *26*, 1603 (1993).
26. Koningsveld R., Solc K.: Collect. Czech. Chem. Commun. *58*, 2305 (1993).